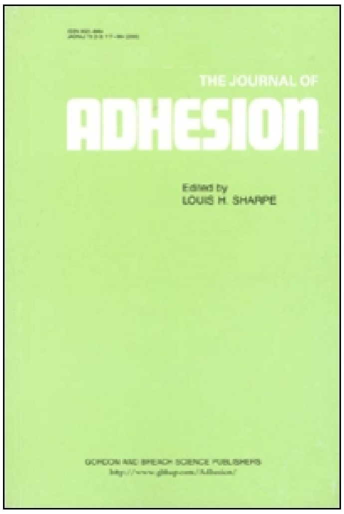

The Journal of Adhesion
Publication details, including instructions for authors and subscription information:
http://www.informaworld.com/smpp/title~content=t713453635

Polymer-Aluminium Adhesion II. Role of the Adhesive and Cohesive Properties of the Polymer

A. Carre[a]; J. Schultz[b]
[a] Centre de Recherches sur la Physico-Chimie des Surfaces Solides, MULHOUSE, France [b] Laboratoire de Recherches sur la Physico-Chimie des interfaces de l'Ecole Nationale Supérieure de Chimie de Mulhouse 3, MULHOUSE CEDEX, France

To cite this Article Carre, A. and Schultz, J.(1984) 'Polymer-Aluminium Adhesion II. Role of the Adhesive and Cohesive Properties of the Polymer', The Journal of Adhesion, 17: 2, 135 — 155
To link to this Article: DOI: 10.1080/00218468408079671
URL: http://dx.doi.org/10.1080/00218468408079671

J. Adhesion, 1984, Vol. 17, pp. 135–156
0021-8464/84/1702-0135 $18.50/0

Printed in the United Kingdom

Polymer-Aluminium Adhesion II. Role of the Adhesive and Cohesive Properties of the Polymer

A. CARRE

Centre de Recherches sur la Physico-Chimie des Surfaces Solides, CNRS
24, avenue du Président Kennedy, 68200 MULHOUSE (France)

J. SCHULTZ

Laboratoire de Recherches sur la Physico-Chimie des Interfaces de
l'Ecole Nationale Supérieure de Chimie de Mulhouse
3, rue Alfred Werner, 68093 MULHOUSE CEDEX (France)

(*Received March 19, 1984; in final form April 28, 1984*)

The study of the adhesive strength of model elastomer/treated aluminium assemblies has led us to propose a new model of the adhesion of viscoelastic materials. In this model the energy of separation of an assembly is described by a product of three terms:

—the reversible energy of adhesion or cohesion,
—a macroscopic dissipation factor due to viscoelastic losses,
—a molecular dissipation factor related to the degree of cross linking of the elastomer.

This new approach allows us to explain the wide range of strengths observed depending on the nature of the surface treatment of the metal substrate. It is suggested that these large differences are essentially due to a variation of the degree of cross linking of the elastomer in the vicinity of the interface.

INTRODUCTION

The subject of adhesion covers a wide variety of concepts and ideas difficult to reconcile and even apparently contradictory depending, for example, on whether a microscopic or a macroscopic stand-point is taken. In this study particular attention has been paid to the molecular aspect of failure by considering model aluminium/elastomer assemblies.

In a former publication,[1] the thermodynamic parameters characterizing the solid surfaces have been determined. We now tackle the fundamental question of the relationship between the experimental strength measured by fracture tests of aluminium/elastomer assemblies and intrinsic properties, such as surface energy, roughness and porosity of the aluminium and surface properties of the polymer.

In addition, the failure being cohesive in many cases, the role of cohesive properties of the polymer in the facture zone was also examined.

On one hand, model assemblies consisting of treated aluminium and SBR or NBR elastomers have been studied by peel tests. On the other hand, the cohesive properties of the same elastomers have been determined either by peeling cloth strip impregnated with the elastomer or by tearing experiments.

MATERIALS

The substrate is a 5052 laminated aluminium. Among the surface treatments considered in the first part of this study,[1] we selected three:

—conversion by phosphatization:

This treatment involves amorphous phosphatization of aluminium surface by a mixture of phosphoric and chromic acids. This leads to a high dispersive component of the surface energy together with a low surface polarity.

—non-sealed sulphuric anodization:

The second treatment corresponds to anodization of the aluminium in sulphuric acid. A freshly treated surface is porous and presents a high surface energy.

—sealed anodization:

The porosity of the anodized surface can be reduced by a subsequent sealing in boiling water in the presence of salts. This operation confers to the aluminium an intermediate value of surface energy.

The elastomers SBR and NBR were chosen mainly because their well-known rheological behaviour facilitates the interpretation of the phenomena occurring during the failure of the joint. The SBR is a 40/60 styrene/butadiene rubber of molecular weight 8.5×10^4 g.mole^{-1} (SBR 1516, Polysar). The NBR is a 34/66 acrylonitrile/butadiene rubber of molecular weight 3.1×10^4 g.mole^{-1} (NBR Perbunan N 3307 NS, Bayer). Their glass transition temperatures (T_g) determined by differential scanning calorimetry (DSC) are -35°C and -26°C respectively.

Their surface energies were determined by classical contact angle measurements. Table I shows the different values of dispersive and polar components, γ_S^D and γ_S^P, of the surface free energies of the elastomer and aluminium surfaces.

TABLE I
Surface energies of the solids (mJ.m^{-2})

Solid	γ_S^D	γ_S^P	γ_S
SBR	29.5	0.5	30
NBR	26.5	9.5	36
Phosphated Al	150	1.5	151.5
Anodized Al	125	44	169
Sealed anodized Al	41	15	56

EXPERIMENTAL

a) Preparation and testing of model assemblies

The model assemblies consisting of an elastomer layer of 1 mm thickness between the aluminium substrate and a cotton fabric were realized by pressing under 5×10^6 Pa at 90°C. The fabric limits the longitudinal elongation of the elastomer during the peel test. The elastomer was slightly crosslinked by incorporating 1.6% wt. of peroxide (1,1 di-t-butylperoxy 3,3,5 trimethylcyclohexane) and maintaining the assembly at 150°C for 50 min under the same pressure.

The values of the molecular weight between cross links, M_c, determined by swelling measurements are 1.2×10^4 and 2.1×10^4 g.mole^{-1} for SBR and for NBR respectively.

The strength of the joint was measured by a 180° peel test. The force, F, necessary to separate the elastomer layer from the aluminium substrate was measured with a dynamometer. The failure energy, $\mathscr{W}$, required to separate unit interfacial area is given by the relationship:

$$\mathscr{W} = \frac{2F}{\omega} \tag{1}$$

where ω is the width of the test strip.

The peel strips were of 2 cm width and 12 cm length.

b) **Determination of the cohesive properties of elastomers**

In order to determine the cohesive strength of the elastomer, samples were prepared as in a) by replacing the aluminium substrate by a cotton cloth strip. Peeling of these samples always leads to a cohesive failure in the elastomer and allows the energy of cohesion of the elastomers to be calculated from relationship (1).

This energy of cohesion was also determined by tearing using a trousers sample of 2 cm width and 0.1 cm thickness, the longitudinal elongation of the legs being limited by using a cotton cloth as in a). The fracture energy, $\mathscr{C}$, is calculated according to the Rivlin and Thomas' relationship:[2]

$$\mathscr{C} = \frac{2F}{e} \tag{2}$$

where F is the tear force and e the length of the tear path. This length depends on the orientation of the fracture plane.

RESULTS

By using the peel test and the samples described above, the strength of aluminium/elastomer assemblies was measured at 20°C in air for a large range of separation rates from 4.2×10^{-6} to 4.2×10^{-3} m.s.$^{-1}$ (i.e. 0.25 to 250 mm.min^{-1}).

First of all, it should be recalled that the peel test leads to two essential pieces of information:

—the locus of failure
—and the energy of separation, $\mathscr{W}$.

These two data are complementary and should not be dissociated.

a) Locus of failure for aluminium/elastomer assemblies

Visual examination of aluminium surfaces after detachment is not sufficient for determining exactly the failure mode (cohesive or interfacial). In particular, when the failure seems to be interfacial or adhesive, it is necessary to have recourse to sensitive techniques of surface analysis, since the residual quantity of either adherent phase might be very small.[3,4]

A simple method was used which consists of comparing the wettability of adherends by a liquid both before the interfacial contact and after failure, the presence of one molecular layer being sufficient to modify the contact angle of the liquid on the solid surface.

In Table II, the values of the contact angles of water on the aluminium surfaces before assembly and after failure are given as are the contact angles on the two elastomers.

TABLE II
Locus of failure by wettability measurements. Contact angles of water on the solids before and after separation

	Surface		θ_{H_2O} ($\pm$ 1 degree)
Initial surfaces	SBR		98
	NBR		74.5
	Phosphated Al		40
	Anodized Al		0
	Sealed anodized Al		54
Al surfaces after separation from	SBR	Phosphated Al	92.5
		Anodized Al	>98*
		Sealed anodized Al	52
	NBR	Phosphated Al	73
		Anodized Al	/**
		Sealed anodized Al	59

*In this case, θ_{H_2O} is a function of the roughness of the residual elastomer layer.

**This substrate underwent irreversible bending during the peel test so that contact angle measurements were not possible due to the curvature of the aluminium surface.

From these data, it can be easily settled that the failure is interfacial for the systems constituted of the low surface energy substrate, *i.e.*, sealed anodized aluminium and cohesive for the systems constituted of high surface energy solids, *i.e.*, phosphated and anodized aluminium (Table III).

These conclusions have been confirmed by scanning electron microscopy analysis.

TABLE III
Observed failure mode for aluminium/elastomer assemblies

Assembly	Failure mode
Phosphated Al/SBR or NBR	cohesive
Anodized Al/SBR or NBR	cohesive
Sealed anodized Al/SBR or NBR	adhesive

b) Energy of separation

Figure 1 represents the variation of the failure energy, $\mathscr{W}$, as a function of the peel rate, R, for sealed anodized aluminium/SBR or NBR assemblies (adhesive failure).

Figures 2 and 3 give the variation of $\mathscr{W}$ for anodized and phosphated aluminium in contact with SBR (Fig. 2) and NBR

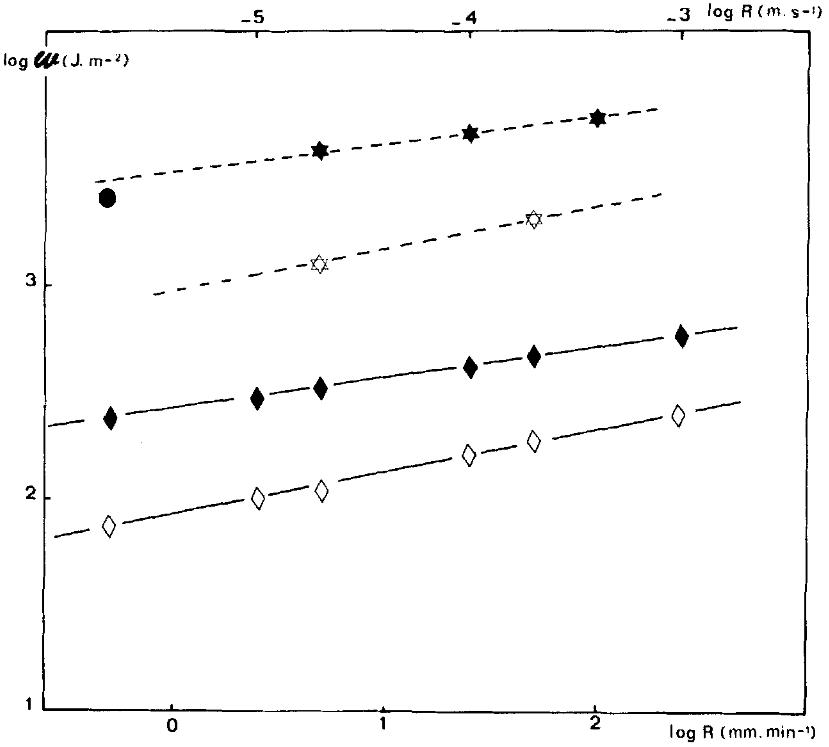

FIGURE 1 $\mathscr{W}$ vs. R for sealed anodized aluminium/SBR (◇) and NBR (◆) assemblies (Interfacial failure); and for bulk SBR (✡) and NBR (✶) measured by peeling.

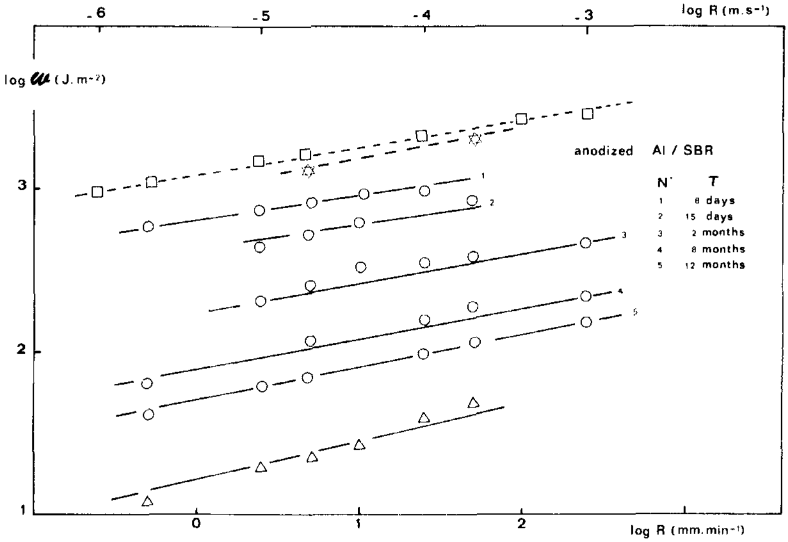

FIGURE 2 $\mathscr{W}$ vs. R for SBR/phosphated aluminium (△) and anodized aluminium (○) assemblies (cohesive failure); and for bulk SBR measured by tearing (□) and peeling (✡).

(Fig. 3). Another parameter studied is the aging time, τ, before interfacial contact is achieved in the case of the anodized aluminium substrate.

For comparison, the cohesive failure energies of the rubbers measured by the cohesive peel test or by tearing are also shown in these three figures.

From these experimental data, several conclusions can be drawn:

—Whatever the system considered, the energy of failure increases when the peel rate increases. This is due to the viscoelastic behaviour of the rubbers, the hysteretic character of the rubber increasing with increasing rate of deformation. Let us also note that the curves are all parallel for a given elastomer.

—Whatever the substrate, the NBR always leads to the highest failure energy at any given peel rate. The reason may be either its important surface polarity or a more dissipative character (lower rate of crosslinking or higher T_g).

—The failure energy of anodized aluminium/elastomer samples decreases drastically with the aging time of the anodized substrate, τ,

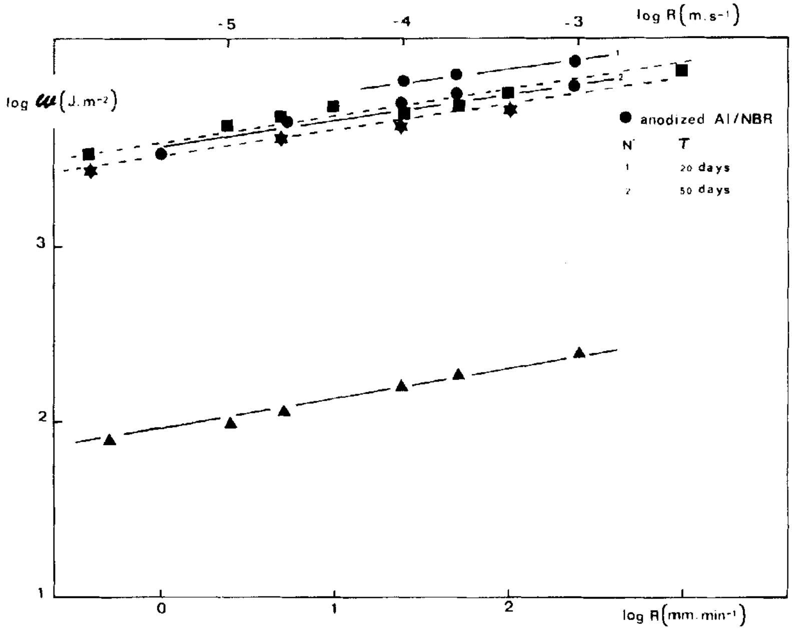

FIGURE 3 $\mathscr{W}$ vs. R for NBR/phosphated aluminium (▲) and anodized aluminium (●) assemblies (cohesive failure); and for bulk NBR measured by tearing (■) and peeling (✦).

before assembly. This is connected to the natural sealing of the porous oxide layer in the presence of atmospheric humidity, the samples having been kept under a 60% RH controlled atmosphere. This natural sealing slowly reduces the depth of the pores.[5] However, this phenomenon does not change the mode of failure (always cohesive in the elastomer). The progressive sealing leads to a decrease of the penetration depth of the polymer in the porous oxide. This penetration of polymers in anodic oxides has been clearly shown in the past[6,7] and by ourselves.[5] The driving force pulling the polymer in the melted state into the pores is due to a capillary phenomenon.

It must be noted that an anodized aluminium surface aged for only 8 days leads to a failure energy very close to the cohesion energy of the bulk elastomer as measured by both peeling and tearing.

After aging for 12 months, it is observed that the failure energy is reduced by a factor of 11 although the failure is still cohesive within the elastomer. Moreover the failure energy of this highly aged sample is still two to three times higher than the one of the phosphated aluminium/SBR sample.

It appears thus that although the failure is cohesive in the elastomer the failure energy may vary over a very large range. For instance, the failure energy of the phosphated aluminium/SBR sample is about 50 times smaller than the cohesive energy of failure of the bulk SBR.

It is also interesting to note that interfacial failure can lead to a higher failure energy than that observed for cohesive failure. This is the case for SBR on sealed anodized aluminium which is about six times higher than on phosphated aluminium as shown on Figure 4.

All these observations led us to examine the theories of interfacial and cohesive failure in order to explain such considerable differences in behaviour.

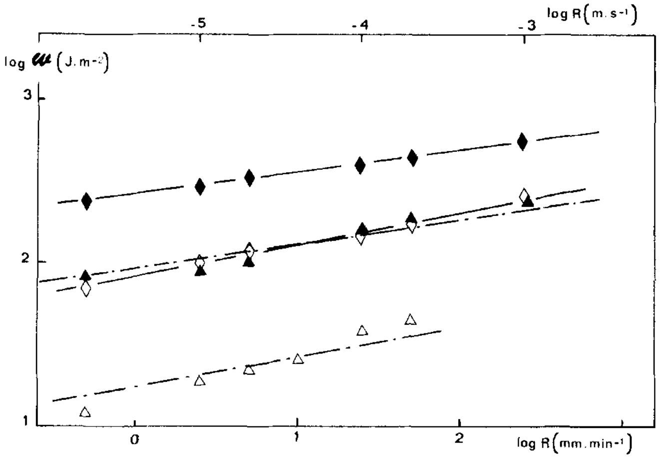

FIGURE 4 $\mathscr{W}$ vs. R for sealed anodized aluminium/SBR (▲) and NBR (◆) (interfacial failure); and for phosphated aluminium/SBR (△) and NBR (◇) cohesive failure).

ANALYSIS OF FAILURE PHENOMENA—A TENTATIVE GENERAL THEORY

a) Interfacial failure

For interfacial failure, Gent and Schultz[8,9] have shown that the failure energy, $\mathscr{W}$, can be expressed as the product of two terms:

$$\mathscr{W} = W_o^a \times f(R) \tag{3}$$

W_o^a is the reversible energy of adhesion related to the surface energies of the solids in contact, S_1 and S_2, through Dupre's equation:

$$W_o^a = \gamma_{S_1} + \gamma_{S_2} - \gamma_{S_1S_2} \tag{4}$$

$\gamma_{S_1S_2}$ being the interfacial energy between the two solids.

$f(R)$ is a mechanical factor corresponding to the dissipation of energy resulting from irreversible deformation of the bulk elastomer. For a given temperature this factor depends only on the rate of separation and on the test geometry.

In conditions close to equilibrium, *i.e.*, in the absence of viscoelastic losses, $\mathscr{W}$ should reach a value of W_o^a of the order of 0.1 $J.m^{-2}$. However, numerous experiments at very low rates of separation or high temperatures (10–14) show that this value is never attained in practice.

b) **Cohesive failure**

In this case the failure energy can be described by a relationship similar to (3) by introducing the reversible energy of cohesion of the elastomer.

In a first step the reversible energy of cohesion, W_o^c, can be considered as resulting from physical interactions, $W_o^c{}_{\text{phys}}$, equal to twice the surface energy of the elastomer, and from chemical interactions (or entanglements), $W_o^c{}_{\text{chem}}$:

$$W_o^c = 2\gamma_S + W_o^c{}_{\text{chem}} \tag{5}$$

Therefore: $$W_o^c > 2\gamma_S \tag{6}$$

By considering that the failure propagates in the weakest part of the assembly either at the interface or cohesively in the elastomer, it is possible to determine the maximum and minimum values of the reversible energies of cohesion of the two elastomers. Table IV presents the reversible energies of adhesion and cohesion calculated from the surface energies as well as the observed mode of failure.

The values of Table IV lead to the following inequalities:

$$\left.\begin{array}{l}\text{for SBR}: 0.076 < W_o^c < 0.130\ (J.m^{-2})\\ \text{for NBR}: 0.088 < W_o^c < 0.134\ (J.m^{-2})\end{array}\right\} \tag{8}$$

TABLE IV
Reversible energies of adhesion and cohesion ($J.m^{-2}$)

	Al/SBR			Al/NBR		
Substrate	W_o^{a}*	W_o^{c}	Failure mode	W_o^{a}*	W_o^{c}	Failure mode
Phosphated Al	0.133	>0.060	cohesive	0.134	>0.072	cohesive
Anodized Al	0.130	>0.060	cohesive	0.156	>0.072	cohesive
Sealed anodized Al	0.076	>0.060	adhesive	0.088	>0.072	adhesive

* W_o^a has been calculated using the relationship of Owens and Wendt:[15] $W_o^a = 2(\gamma_{S1}^D \gamma_{S2}^D)^{1/2} + 2(\gamma_{S1}^P \gamma_{S2}^P)^{1/2}$ (7)

The contribution of the chemical bonds, $W_o^c{}_{\text{chem}}$, can therefore be evaluated from relations (5) and (8):

$$\left.\begin{array}{l}\text{SBR}: 0.016 < W_o^c{}_{\text{chem}} < 0.070\ (\text{J.m}^{-2})\\ \text{NBR}: 0.016 < W_o^c{}_{\text{chem}} < 0.062\ (\text{J.m}^{-2})\end{array}\right\} \tag{9}$$

It appears from these simple considerations that the contribution of the chemical interactions to the reversible energy of cohesion of the elastomer are at most of the same order of magnitude as the physical interactions contribution.

However, the term $W_o^c{}_{\text{chem}}$ can be calculated more precisely by considering the number of C-C bonds "reversibly" broken during the failure process using the following relationship:

$$W_o^c{}_{\text{chem}} = \nu \times \text{u} \tag{10}$$

ν represents the number of broken chains per unit area of failure plane and u the energy of dissociation of an elementary C-C bond, i.e. 5×10^{-19} J.[16]

The parameter υ can be calculated by using the following models:

α) Calculation using Vincent's model.

Vincent[17] relates ν to the polymer density, d, the length, l, and the weight, m, of a monomer unit:

$$\nu = \frac{dl}{m} \tag{11}$$

A value of $2 \times 10^{18}.\text{m}^{-2}$ has been obtained by Vincent in the case of polybutadiene which would lead to a value of $W_o^c{}_{\text{chem}}$ of the order of 1 J.m^{-2}.

However this model does not take into account the fact that C-C bonds of the same chain may cross the fracture plane. Therefore, this approach leads to an overestimation of the number of broken bonds. Moreover in Vincent's relation ν appears to be independent of the degree of crosslinking of the elastomer.

β) Calculation using Lake and Thomas' model

According to Lake and Thomas,[18] the energy of dissociation of the C-C bonds crossing the fracture plane is not the only one to intervene. As a matter of fact, in order to break one C-C bond it is necessary to stretch almost up to the breaking point all the bonds in a chain between two crosslinks. The energy stored in the chain is irreversibly dissipated when one of these C-C bonds is broken. This model leads to the concept of a threshold value, $\mathscr{C}_o$, of the energy of cohesion which can be measured experimentally in the absence of macroscopic viscoelastic losses. $\mathscr{C}_o$ is given by:

$$\mathscr{C}_o = v \times u \times n \tag{13}$$

where n is the number of C-C bonds in a chain between two crosslinks.

In equation (13) the number of chains crossing the unit fracture plane, v, is calculated from the theory of elasticity according to:

$$v = (\frac{2}{3\pi}\bar{n})^{1/2}\, \gamma l\, N \tag{14}$$

where $\bar{n}$ is the number of monomer units per chain, γ is a factor determined by the freedom of rotation about bonds in the chain and is related to the flexibility, l is the length of a monomer unit and N the number of chains per unit volume.

Finally $\mathscr{C}_o$ is expressed as a function of M_c:[18]

$$\mathscr{C}_o = kM_c^{1/2} \tag{15}$$

Factor k is roughly equal to 0.3 $\mathrm{J.m^{-2}.(g.mole^{-1})^{1/2}}$ for almost all elastomers.[16]

All the experimental determinations of the energy of failure of elastomer in near-equilibrium conditions are in good agreement with this theory.[19,23] For the SBR and NBR elastomers studied here, the values of $\mathscr{C}_o$ calculated using equation (15) are respectively 33 and 43 $\mathrm{J.m^{-2}}$. The value determined directly from tear experiments is of the order of 100 $\mathrm{J.m^{-2}}$ for SBR which is in fairly good agreement with the value calculated from the theory of Lake and Thomas.

Further, the number of C-C bonds broken per unit area can be calculated using equation (13), *i.e.*:

$$v = \frac{\mathscr{C}_o}{n \times u} \tag{16}$$

For SBR, n is about 620 given that, the molecular weight between crosslinks, M_c, is of the order of 1.2×10^4 $\mathrm{g.mole^{-1}}$, the chain consisting of 130 butadiene units and 50 styrene units. v is therefore equal to 10.6×10^{16} $\mathrm{bonds.m^{-2}}$.

The same calculation for NBR leads to a value of v equal to 6.9×10^{16} $\mathrm{bonds.m^{-2}}$.

According to equation (10) the chemical contributions to the reversible energy of cohesion of SBR and NBR, $W_o{}^c{}_{\mathrm{chem}}$, are respectively 0.050 and 0.035 $\mathrm{J.m^{-2}}$.

Thus it can be shown that this calculated contribution due solely to the rupture of chemical bonds not taking into account the deformation of the bonds in the chain is of the same order of magnitude as the physical contribution ($W_o{}^c{}_{\text{phys}} = 2\gamma_S$) and is in excellent agreement with the inequalities (9) established from the locus of failure.

γ) Calculation using network models

i) Bueche's model

Bueche[24] considers a three-dimensional reticulate network of crosslinked chains. The number v of chains crossing the unit plane is equal to:

$$v = \frac{(\mathrm{d}.\mathcal{N})^{2/3}}{3M_c} \tag{17}$$

where d is the density of the elastomer.

Again from this model and according to equation (10), the values of $W_o{}^c{}_{\text{chem}}$ can be determined, *i.e.*:

for SBR, $W_o{}^c{}_{\text{chem}} = 0.033\ \mathrm{J.m^{-2}}$
for NBR, $W_o{}^c{}_{\text{chem}} = 0.022\ \mathrm{J.m^{-2}}$

ii) Flory and Rehner's model

This model is based on a homogeneous distribution of the crosslinks in a tetrahedric network.[25] As a consequence, the crosslinks may be considered to be in a face centred cubic system.

The number v of chains crossing a unit plane parallel to one of the face of the cube is equal to:[5]

$$v = \frac{(d.\mathcal{N})^{2/3}}{2M_c} \tag{18}$$

This leads to the following values for $W_o{}^c{}_{\text{chem}}$:

for SBR, $W_o{}^c{}_{\text{chem}} = 0.042\ \mathrm{J.m^{-2}}$
for NBR, $W_o{}^c{}_{\text{chem}} = 0.029\ \mathrm{J.m^{-2}}$

These two series of values are of the same order of magnitude as that calculated from the model of Lake and Thomas and again satisfy the inequalities (9).

All the calculated chemical contributions of the reversible energies of cohesion of SBR and NBR are summarized in Table V.

TABLE V
Chemical contribution to the reversible energy of cohesion, $W_{o\,\mathrm{chem}}$ ($\mathrm{J.m^{-2}}$)

		$W_o{}^c{}_{\mathrm{chem}}$ calculated using:			
Elastomer	Inequalities (9) Limiting values	Model of Vincent (11)	Model of Lake and Thomas (16)	Model of Bueche (17)	Model of Flory and Rehner (18)
SBR	0.016–0.070	0.90	0.050	0.033	0.042
NBR	0.016–0.062	1.10	0.035	0.022	0.029

c) **A tentative general theory**

The energy of cohesion, $\mathscr{C}$, as measured by a tear test can be expressed as a product of two terms:

$$\mathscr{C} = \mathscr{C}_o \times f(R) \tag{19}$$

where $\mathscr{C}_o$ is the threshold value of the measured energy of cohesion and $f(R)$ the viscoelastic dissipation function.

According to the theory of Lake and Thomas, $\mathscr{C}$ can also be expressed by:

$$\mathscr{C} = W_o{}^c{}_{\text{chem}} \times n \times f(R) \tag{20}$$

However, we have shown that $W_o{}^c{}_{\text{chem}}$ is of the same order of magnitude as $W_o{}^c{}_{\text{phys}}$, therefore we propose to combine the two terms in one, $W_o{}^c$, describing all the physical and chemical interactions. The equation (20) can therefore be written:

$$\mathscr{C} = W_o{}^c \times g(M_c) \times f(R) \tag{21}$$

In the more general case of a separation test where the failure is cohesive within the elastomer, this equation will be rewritten:

$$\mathscr{W} = W_o{}^c\, g(M_c)\, f(R) \tag{22}$$

where $\mathscr{W}$ in the measured energy of separation, $W_o{}^c$ is the reversible energy of cohesion, $g(M_c)$ is a factor of molecular dissipation equal to the number of C-C bonds between two crosslinks, and $f(R)$ the factor of macrocopic or viscoelastic dissipation.

The product $W_o{}^c\, g(M_c)$ is equal to the threshold value $\mathscr{C}_o$.

The introduction of the physical term, $W_o{}^c{}_{\text{phys}}$, in the reversible energy of cohesion, $W_o{}^c$, is at least partly justified by the fact that the value of $\mathscr{C}_o$ calculated according to this hypothesis is very close to the ones determined experimentally by tearing. $\mathscr{C}_c$ is now defined by the following relationship:

$$\mathscr{C}_o = (2\gamma_S + W_o{}^c{}_{\text{chem}}) \times g(M_c) \tag{23}$$

with $g(M_c) = n$.

Equation (23) leads to values of 62 and 130 J.m^{-2} for SBR and NBR respectively.

Let us now consider that the same molecular dissipation mechanism develops in the case of interfacial failure in order to explain the considerable differences between threshold values of the energy of separation, and calculated reversible energies of adhesion.[10-14]

By analogy with equation (23) we can write:

$$\mathscr{C}_o{}^a = W_o{}^a \times g(M_c) \tag{24}$$

This time, $\mathscr{C}_o{}^a$ represents the threshold value of the energy of separation as measured in near equilibrium conditions, *i.e.* at low rates of separation and/or high temperatures; $W_o{}^a$ is the reversible energy of adhesion as defined by Dupre when only physical interactions are exchanged at the interface.

We are aware that this theory is based on an unproved assumption that is that the same molecular dissipation factor applies whatever the energy of the bond. As a matter of fact, the molecular dissipation term $g(M_c)$ should be regarded with caution in the case of purely physical interactions of low energy. In this case $g(M_c)$ could take on all values between 1 (no molecular dissipation) and the actual value of $g(M_c)$.

DISCUSSION

Relation (22) clearly demonstrates that for a given elastomer there are two parameters which determine the threshold value of the energy of separation:

—the reversible energy of adhesion or cohesion, W_o, which represents the energy needed to break "reversibly" the bonds crossing the fracture plane at the interface or in the bulk elastomer,

—the length of the chains crossing this plane or ending in this plane.

a) *Cohesive failure*: Comparison of anodized and phosphated aluminium/elastomer assemblies (Fig. 2 and 3).

Since the experimental curves log $\mathscr{W}$ *vs.* log R are parallel which means that the mechanical factor $f(R)$ is constant, the difference in failure energy between anodized and phosphated aluminium must be due to a difference in $\mathscr{C}_o$. Therefore, taking as a reference the experimental value of $\mathscr{C}_o$ relative to the failure of the bulk elastomer, *i.e.* $\mathscr{C}_{oref} = 100\ \mathrm{J.m^{-2}}$ for SBR, the curves in Figure 2 together with relationship (22) allow us to calculate $\mathscr{C}_o$ for the different SBR/aluminium assemblies, knowing that:

$$\frac{\mathscr{W}}{\mathscr{W}_{ref}} = \frac{\mathscr{C}_o}{\mathscr{C}_{oref}}$$

(24) (at any given value of R)

These calculated values of $\mathscr{C}_o$ are reported in Table VI.

TABLE VI
Threshold values $\mathscr{C}_o$ for the cohesive failure of SBR/aluminium assemblies. Calculated values of M_c in the fracture zone

Assemblies	$\mathscr{C}_o$ (J.m^{-2})	M_c (g.mole^{-1})
SBR/SBR (cloth)	100	12,000
SBR/anodized Al, = 8 days	63	7,500
SBR/anodized Al, = 15 days	42	5,000
SBR/anodized Al, = 2 months	18	2,200
SBR/anodized Al, = 8 months	9	1,100
SBR/anodized Al, = 12 months	6	700
SBR/phosphated Al	2.5	240

Simple considerations show that the reversible energy of cohesion, W_o^c, cannot vary over a large range and is therefore not able to explain the large variation of $\mathscr{C}_o$ reported in Table VI. It is concluded that the phenomenon responsible for this observation is related to the length of the chains in the fracture zone. This is clearly seen in the following examples comparing the $\mathscr{C}_o$ value of SBR obtained by tear experiments ($\mathscr{C}_o = 100$ J.m^{-2}) and the $\mathscr{C}_o$ value of SBR calculated from the peeling experiments of SBR/phosphated aluminium assemblies ($\mathscr{C}_o = 2.5$ J.m^{-2}).

According to equation (23) it follows that

$$\frac{g(M_c)}{g(M_c')} = 50,$$

and therefore: $M_c' = \dfrac{12{,}000}{50} = 240$ g.mole^{-1}

The values of M_c of the elastomer in the fracture zone calculated following this same approach (admitting that W_o^c is constant and of the order of 0.10 J.m^{-2}) are reported in Table VI.

It is of utmost importance to note that in the case of the SBR/aged anodized aluminium the fracture surface gets closer to the interface when the sealing of the pores increases, *i.e.*, when the time of aging increases. It is observed in Table VI that the value of M_c decreases at the same time. It can therefore be concluded that there is a gradient of the degree of crosslinking, M_c being of the order of 12,000 g.mole^{-1} in the bulk elastomer and reaching 240 g.mole^{-1} near the interface.

The same observation can be made for the NBR based assemblies,

M_c varying from a value of 21,000 g.mole^{-1} in the bulk to a value of 700 g.mole^{-1} in the vicinity of the interface.

These findings are in good agreement with the theory of weak boundary layers of Bikerman.[26] It must be noted however that paradoxically this "weak boundary layer" results from a higher degree of crosslinking of the elastomer near the interface. Whether this is due to a migration of the low molecular weight fraction of the elastomer to the interface or to the intervention of the aluminium surface in the crosslinking kinetics is still open to conjecture.

b) *Adhesive failure*: Case of sealed anodized aluminium/elastomer assemblies (Fig. 1).

Again in this case the comparison of the tear energy of SBR and the energy of separation of sealed anodized aluminium/SBR samples leads to:

$$\mathscr{W}_{\mathrm{SBR/Al}} = \mathscr{C}_o^a \times f(R) \frac{\mathscr{W}_{\mathrm{SBR/Al}}}{W_{\mathrm{SBR/SBR}}} = 0.1 \text{ (Fig. 1)}$$

$$\mathscr{W}_{\mathrm{SBR/SBR}} = \mathscr{C}_{o\mathrm{SBR}} \times f(R)$$

$$\frac{\mathscr{W}_{\mathrm{SBR/Al}}}{\mathscr{W}_{\mathrm{SBR/SBR}}} = \frac{\mathscr{C}_o^a}{\mathscr{C}_{o\mathrm{SBR}}} = \frac{W_o^a \times g(M_c')}{W_o^c \times g(M_c)}$$

$$= \frac{W_o^a \times M_c'}{W_o^c \times M_c}$$

$$i.e.\text{: } M_c' = \frac{\mathscr{W}_{\mathrm{SBR/Al}}}{W_{\mathrm{SBR/SBR}}} \times \frac{W_o^c}{W_o^a} \times M_c$$

A value of 1,600 g.mole^{-1} is found at the interface sealed anodized aluminium/SBR. The same calculation applied to the sealed anodized aluminium/NBR leads to a value of $M_c' = 2{,}000$ g.mole^{-1}.

Although the model established for cohesive failure applies to adhesive failure only to a first approximation as stated previously it can however be tentatively concluded that the formation of a weak boundary layer due to a higher crosslinking density occurs also when the elastomer is in contact with the low energy surface but to a smaller extent.

As an illustration let us note that the molecular weight of the chains near the interface with the phosphated aluminium ($\gamma_S = 150$ mJ.m^{-2}) is about 50 times smaller than in the bulk, whereas it is only 8 times smaller when in contact with the sealed anodized aluminium ($\gamma_S = 50$ mJ.m^{-2}).

CONCLUSION

The extensive study of aluminium/elastomer assemblies shows that depending on the nature of the surface treatment of the metal, the failure can be either adhesive or cohesive and the energy of separation varies over a large range. To explain all the observations, a general theory of adhesion of viscoelastic materials has been tentatively established. According to this model the energy of separation, $\mathscr{W}$, as measured by a peel test may be expressed as a product of three terms:

$$\mathscr{W} = W_o \times g(M_c) \times f(R)$$

where W_o is the reversible energy of adhesion or cohesion measuring the energy required to break all physical and chemical bonds per unit area of the fracture plane, $g(M_c)$ is a molecular dissipation factor related to the irreversible deformation of the bonds in the chain between two crosslinks. This term is in fact equal to the number of C-C bonds in the elementary chain. $f(R)$ is a macroscopic dissipation factor related to the hysteretic properties of the bulk elastomer.

The product $W_o \times g(M_c)$ is represented by $\mathscr{C}_o$ and refers to the threshold value of the energy of separation when measured at equilibrium.

This general theory has suggested that a gradient of degree of crosslinking of the elastomer exists in the immediate vicinity of the interface, the degree of crosslinking being higher near the interface than in the bulk. This effect is comparable to the formation of a weak boundary layer.

This explains why the measured energy of separation of the different assemblies studied varies considerably even when the failure is cohesive within the elastomer and why the energy of separation in the case of interfacial failure can be superior to that of cohesive failure.

References

1. A. Carre, J. Schultz, *J. Adhesion* **15**, 151 (1983).
2. R. S. Rivlin, A. G. Thomas, *J. Polym. Sci.* **10**, 291 (1953).
3. D. M. Wyatt, R. C. Gray, J. C. Carver, etc. *Appl. Spectroscopy* **28**, (5), 439 (1974).
4. W. L. Baun, in *Adhesion Measurement of Thin Films, Thick Films and Bulk Coatings*, ASTM STP 640, K. L. Mittal Ed. (ASTM, Philadelphia, 1978), p. 41.
5. A. Carre, Thèse de Doctorat d'Etat, Université de Haute-Alsace, Mai 1980.
6. K. Bright, B. W. Malpass, D. E. Packham, *Br. Polym J.* **3**, 205 (1971).

7. D. E. Packham, K. Bright, B. W. Malpass, *J. Appl. Polym. Sci.* **18**, 3237 (1974); *ibid* **18**, 3249 (1974).
8. A. N. Gent, J. Schultz, *J. Adhesion* **3**, 281 (1973).
9. J. Schultz, A. N. Gent, *J. Chim. Phys.* **70** (5), 708 (1973).
10. A. N. Kuskin, L. M. Sergeeva, Yu.S. Lipatov, *J. Adhesion* **6**, 275 (1974).
11. A. Ahagon, A. N. Gent, *J. Polym. Sci., Phys. Ed.* **13**, 1285 (1975).
12. A. N. Gent, G. R. Hamed, *Plastics and Rubber: Materials and Applications*, February, 17 (1978).
13. M. F. Vallat, Thèse de Doctorat, Université de Haute-Alsace, Février 1979.
14. A. N. Gent, *Adhesives Age*, February, 27 (1982).
15. D. K. Owens, R. C. Wendt, *J. Appl. Polym. Sci.* **13**, 1741 (1969).
16. A. N. Gent, *Science and Technology of Rubber*, F. R. Eirich (Acad. Press. New York, 1978), p. 427.
17. P. I. Vincent, *Polymer* **13**, 558 (1972).
18. G. J. Lake, A. G. Thomas, *Proc. Roy. Soc., London* **A300**, 103 (1967).
19. G. J. Lake, P. B. Lindley, *J. Appl. Polym. Sci.* **9**, 1233 (1965).
20. E. H. Andrews, *Makromol. Chem. Suppl.* **2**, 189 (1979).
21. H. K. Mueller, W. G. Knauss, *Trans. Soc. Rheol.* **15**, 217 (1971).
22. A. Ahagon, A. N. Gent, *J. Polym. Sci.; Phys. Ed.* **13**, 1903 (1975).
23. A. N. Gent, R. H. Tobias, *ACS Symp. Ser.* (*Elastomers, Rubber, Elasticity*) (Am. Chem. Socy., Washington, DC, 1982), p. 193.
24. F. Bueche, *Physical Properties of Polymers* (Interscience Publishers, New York, 1962), p. 57.
25. L. R. G. Treloar, *Physics of Rubber Elasticity* (Clarendon Press, Oxford, 1967), p. 117.
26. J. J. Bikerman, *Ind. and Eng. Chem.* **59**, 41 (1957).